UC San Diego
UC San Diego Previously Published Works

Title

An investigation of maximum particle velocity as a universal invariant-Defined by a statistical measure of failure or plastic energy loss for acoustofluidic applications.

Permalink

Journal

The Journal of the Acoustical Society of America, 150(2)

ISSN

0001-4966

Authors

Singh, Arik
Zhang, Naiqing
Friend, James

Publication Date

2021-08-01

DOI

10.1121/10.0005816

Peer reviewed

An Investigation of Maximum Particle Velocity as a Universal Invariant — Defined by a Statistical Measure of Failure or Plastic Energy Loss for Acoustofluidic Applications

Arik Singh,[1] Naiqing Zhang,[1] and James Friend[1, a]

Medically Advanced Devices Lab, Center for Medical Devices,

Department of Mechanical and Aerospace Engineering, Jacobs School

of Engineering and Department of Surgery, School of Medicine,

9500 Gilman Dr. MC0411, University of California San Diego, La Jolla, CA 92093,

USA

(Dated: 15 June 2021)

Materials under vibration experience internal stress waves that can cause material failure or energy loss due to inelastic vibration. Traditionally, failure is defined in terms of material acceleration, yet this approach has many drawbacks, principally because it is not invariant with respect to scale, type of vibration, nor material choice. Here, the likelihood of failure is instead considered in terms of the maximum vibration or particle velocity for various metals, polymers, and structural materials. The exact relationship between the maximum particle velocity and the maximum induced stress may be derived, but only if one knows the details of the vibration, material, flaws, and geometry. Statistical results with over thousands of individual trials are presented here to demonstrate a wide variety of vibrations across a sufficient variety of these choices. Failure in this context is defined as either fracture or plastic yield, the latter associated with inelastic deformation and energy loss during vibration. If the maximum permissible cyclical stress in material vibration is known, to at least an order of magnitude, the probability of this type of failure may be computed for a range of vibration velocities in each material. The results support the notion that a maximum particle velocity on the order of 1 m/s is a universal and critical limit that, upon exceeding, causes the probability of failure to become significant regardless of the details of the material, geometry, or vibration. We illustrate this in a specific example relevant to acoustofluidics, a simple surface acoustic wave device. The consequences of particle velocity limit analysis can effectively be used in materials and structural engineering to predict when dynamic material particle velocity can cause inelastic losses or failure via brittle fracture, plastic deformation, or fatigue failure.

2

[a]jfriend@ucsd.edu; http://friend.ucsd.edu

I. INTRODUCTION

In the study of acoustic wave propagation in elastic solids, there is a physical limit to how much materials can vibrate before failing. This phenomenon appears across disciplines, from the study of actuating robotics or microelectromechanical (MEMS) devices (Kimberley *et al.*, 2009) to vibration fatigue and crack propagation of complex structures and earthquakes explored by civil engineers and geologists alike (Dehghani and Ataee-Pour, 2011; Mikitarenko and Perelmuter, 1998). If such a physical limit could be found, especially if it were defined in terms of easily measured parameters and the properties of the material being used, the choice of materials and geometry in engineering design could be made simpler. Additionally, finite element modeling of vibrations would be easier, alleviating the need to resort to complex, dynamic stress-strain models to evaluate the risk of failure (Halfpenny, 1999). In a vast majority of cases, vibration and acoustics are carried in physical structures with the aim of avoiding inelastic or plastic deformation, fatigue failure, or fracture in these structures. Here, we assume that any of these phenomena represent structural failure.

For years, the acceleration has been used to describe both the potential and severity of failure due to localized peak stress (Gaberson *et al.*, 2000). Termed *shock severity*, it often is presented (Nwosu *et al.*, 2016; Standard, 1989) as a number of *g*'s, with $g = 9.81$ m/s^2, representing earth's gravitational acceleration. This concept is applied across many disciplines, from petroleum and geological engineering (Zhang and Zhao, 2014) to planetary dynamics (Ramesh *et al.*, 2015) and microdevices (Kimberley *et al.*, 2009), and from the formal literature to data sheets for public consumption. A notable example of the latter among many, the 1.8" hard drive

4

used in the last popular portable music player—Apple's classic iPod—is described by Toshiba as being able to tolerate $2000g$ from a drop and $2g$ vibration at 15–500 Hz while operating (Collins, 2004). Gaberson expressed understandable frustration with this use of acceleration to determine the risk of failure, stating "g's as any kind of shock severity is useless, even in the face of 50 years of tradition".

Due to the direct relationship between strain and displacement in a stress wave, maximum displacement has also been occasionally used to determine the likelihood a given material will fail under vibratory conditions (Hunt, 1960), though it does not often appear in the published literature outside of earthquake research (Cosenza and Manfredi, 2000), where even there it is considered to have modest utility (Hancock and Bommer, 2006).

The particle (or vibration) velocity is a potential alternative to these two choices. Remarkably, it may prove to be the most universal quantity in defining the limiting motions of acoustic wave propagation and vibration in materials. Many years ago, Crandall and Hunt separately (Crandall, 1962; Hunt, 1960) determined that the internal stress and the particle velocity in elastic solids were directly related to each other—to at least an order of magnitude—for a few specific forms of vibration in otherwise flaw-free and continuous structures. Gaberson (Gaberson *et al.*, 2000) defined the closely related *pseudovelocity* (V_0) and claimed it to be the most useful quantity to determine the risk of structural damage due to its vibration. The pseudovelocity is defined (using $\triangleq$) as the maximum displacement multiplied by the angular frequency:

$V_0 \triangleq \omega \max_{x,t} u(x, t) = 2\pi f U_0$ (please consult the glossary of terms in Appendix A).

In fact, the particle velocity can serve to define the risk of failure and changes in observed vibration phenomena that otherwise depend upon stress. The basic idea is to define a *maximum particle velocity* to represent the true limit of structural vibration while avoiding failure.

That the particle velocity is not more widely appreciated and utilized does seem to be a consequence of relying on the acceleration in assessing failure risk, as Gaberson describes, probably from the familiarity of using *g*-loading for predicting static failure. The cleverly presented relationship by Hunt and Crandall (Crandall, 1962; Hunt, 1960) between stress and particle velocity in unflawed structures appears to be forgotten. At the very least, it appears that this relationship has never been applied to a broader range of materials, other forms of structural vibration, nor structures with flaws or significant damping.

In recent years, disciplines such as *acoustofluidics* (Connacher *et al.*, 2018a; Friend and Yeo, 2011) and *ultrasonic actuation* (Watson *et al.*, 2009) have arisen that employ much higher frequency acoustic waves to drive observable motion of fluids, cells, particles, motor components, and so on for a variety of purposes. The desire to produce these results from piezoelectric materials operating at resonance to maximize the energy transformed from electrical to kinetic forms results in very large energies concentrated in small volumes, on the order of 0.1 W in a 100 μm box for short periods. In water or most solids one would consider using in these applications, this represents a specific energy of ~100 MW/kg, remarkably exceeding the specific energy of coal, natural gas, and gasoline (termed *higher heating value* in (Demirbas, 2007)). More energy is trapped in a volume by the mechanical motion induced by high frequency vibration than is released from the same volume by chemical reaction of these common fuels.

6

It should come as no surprise, then, that failure of these devices is widespread, especially in research and development. The motivation of this work is to identify an overall limit to the vibration as a design tool, using the risk of failure—either inelastic vibration giving rise to significant energy loss or outright failure of the material.

In what follows, we seek to identify a maximum practical particle velocity that fulfills these criteria. It turns out that the particle velocity does appear to be a useful tool in judging the risk of a broadly defined "failure" from damping, fatigue, fracture, or plastic yielding across a variety of materials and vibration types.

The paper is organized as follows. We first describe the analysis framework used to determine the limiting particle velocity for avoiding probable material failure. This is followed by an update of the classic concept of a material-defined upper limit to vibration amplitude (Crandall, 1962; Hunt, 1960). By virtue of the Monte Carlo method, we are able to then introduce extensions to this classic concept, taking in turn the effects upon the maximum particle velocity due to changes in the geometry of the structure, the effects of damping, the presence of cracks in brittle materials or stress concentrations in ductile materials, and the peculiar effects of fatigue. We chain these disparate effects together for a sample run, some of them active, others not, as randomly determined for each run. After tens of thousands of runs, it becomes evident that one can indeed define an overall *maximum particle velocity*, a universal, limiting order-of-magnitude for the particle velocity that, when exceeded, will potentially lead to material failure or inelastically-limited vibration with a probability of 50%. For each effect, randomly chosen parameters are selected over defined, reasonable ranges as necessary to produce a so-

lution. The method is extensible, in that the reader can employ the approach for their situation as required to determine the appropriate maximum particle velocity.

II. ANALYTICAL AND STATISTICAL ANALYSIS OF MAXIMUM PARTICLE VELOCITY LIMITS

Our goal in this effort is not to exhaust every possible combination of material, vibration, shape, and failure mode. Instead, we consider specific cases that appear to adequately represent the vast range of options. The Monte Carlo method is then employed to choose, at random: a material, the type and presence of a flaw in the material, the details of the vibration, and a structure carrying the vibration, potentially with geometric constraints. A choice for each of these parameters is made within what we believe to be a reasonable range to define a trial run. This run produces a prediction of the maximum stress present in the structure. This stress may then be compared to the yield stress for the material, corrected to deal with the dynamic nature of the motion and the damping of the material.

The entire aim is to seek a correlation between the order of magnitude of the particle velocity induced in a structure—perhaps with a flaw, significant damping, or constrained geometry— and the overall probability of failure of that material. Using this correlation, we seek to produce an order-of-magnitude estimate for the limiting particle velocity that may exist for a given material, and hopefully for all the materials we have selected for consideration as representatives of most practical engineering materials.

A.   Process of Analysis

125   It will be later shown in subsection II B that an maximum particle velocity $v_{\max}$ may be de-

126   fined as a material property from the material's yield strength, stiffness, and density. Beyond

127   this value, the material's failure is assured. How the material fails depends on the details.

128   The strategy is to first select a representative material: diamond, steel, aluminum, copper,

129   polypropylene (PP), polyvinyl chloride (PVC), polymethyl methacrylate (PMMA), glass, con-

130   crete, or wood. All materials are presumed to be isotropic for tractability, and in realizing the

131   use of anisotropic or composite media affects the material properties, but does not change

132   them by orders of magnitude. These materials represent, broadly, those used in typical engi-

133   neering structures that would be subjected to large amplitude vibration.

134   It is important to note here that mechanical damping is another means to potentially limit

135   the amplitude of vibration or acoustic waves in a structure. Following the classic approach in

136   defining damping, one may define a loss factor for harmonic oscillations, $\eta = D/2\pi W$, where D

137   represents the energy dissipated over each vibration cycle and W represents the combination

138   of the energy stored and introduced into the system over a given cycle (Carfagni *et al.*, 1998).

139   Unlike the damping ratio, the loss factor, η, remains appropriate here even for strongly nonlin-

140   ear systems (Pritz, 1998).

141   In many disciplines, however, the quality factor, Q, is a far more familiar and easily deter-

142   mined measure of the damping present in a given vibration that is responsible for energy loss.

143   The greater the Q, the lower the energy lost to damping (Carfagni *et al.*, 1998). The relationship

between them is often approximated by $Q \approx 1/\eta$, though the full definition is more complex:

$$\frac{1}{Q} \triangleq= \sqrt{1+\eta} - \sqrt{1-\eta}, \tag{1}$$

which may be rearranged and expanded to produce an approximate series relation of the loss factor in terms of the quality factor,

$$\eta = \frac{1}{Q} - \frac{1}{8Q^3} - \frac{1}{128Q^5} + \mathscr{O}\left[\left(\frac{1}{Q^7}\right)\right], \tag{2}$$

where $\mathscr{O}$ is the order of the error in the approximation (Bachmann–Landau notation, (Bachmann, 1894)).

In any case, the ratio of energy lost per cycle, D, to the total energy, W, $D/W \triangleq 2\pi\eta \approx 2\pi/Q$. Notably,

$$\lim_{Q \to 2\pi^+} \frac{D}{W} = 1. \tag{3}$$

The key implication of this result is to recognize that, whatever the nature of the vibration induced in a system, if $Q < 10^1$, the limiting particle velocity is not due to material failure. It is instead governed by the energy loss to damping, and acoustic or vibration energy is dissipated too quickly to sustain vibration. Thus, most rubbers and some plastics are unrealistic choices as they will be limited by their acoustic loss during elastic deformation, instead of a failure criteria which might be due to inelastic deformation or fracture. In this study, all the selected materials exhibit quality factors $Q > 10^1$, a requirement for their selection.

We then choose the form of acoustic wave propagation, noting that it reduces the particle velocity at which failure is guaranteed from the material-defined value $v_{\max}$ to a limiting par-

10

ticle velocity, v_{lim}. In other words, for a particular case defined by the type of acoustic wave and the shape of the structure that carries it, v_{lim} defines the threshold between material integrity and failure. By contrast, the intrinsic threshold between material integrity and failure is always defined by v_{max}. Local stress concentrations, fatigue, fracture toughness, and flaws are responsible for the difference.

We represent the reduction from an ideal v_{max} to v_{lim} as a product

$$v_{\text{lim}} \triangleq \prod_{i=1}^{5} \Psi_{ij} v_{\text{max}}, \tag{4}$$

for the jth case of N total cases. The type of vibration transmitted through the structure as an acoustic wave—for example, longitudinal or transverse waves—reduces the material's maximum particle velocity by a certain amount, defined by Ψ_{1j}. The frequency of the acoustic wave strongly affects the damping and the effective stiffness of the material, which collectively acts to also reduce the limit particle velocity, represented by Ψ_{2j}. The material may also have a flaw, a hole, crack, or similar penetrating geometry, producing a stress concentration that reduces the limit particle velocity v_{lim} even further—by a factor of Ψ_{3j}. We also consider the possibility of ductile failure (with Ψ_{4j}) or fatigue failure (Ψ_{5j}) in reducing the maximum particle velocity to the limiting particle velocity. The relationship is outlined in Fig. 1.

Choosing the material allows us to determine v_{max}. We then define the limit particle velocity as v_{lim} for the jth run such that $j \in \{1, 2, \ldots, N\}$, with $N = 10,000$ here. We note that $v_{\text{lim},j} \leq v_{\text{max}}$ for all j, and define $v_{\text{lim},j} \triangleq \beta_j v_{\text{max}}$ such that $\beta_j \triangleq \prod_{i=1}^{5} \Psi_{ij}$ and $0 \leq \beta_j \leq 1$ for all j, as $0 \leq \Psi_{ij} \leq 1$ for all i, j. The probability, $P_{\text{f}}(v)$ that the selected material will fail for a chosen particle velocity, v, is then determined by pairwise comparing this value to each and every

11

$$v_{\text{lim},j} = \underset{\substack{\text{Case} \\ \text{limit} \\ \text{velocity}}}{\Psi_{1j}} \cdot \underset{\substack{\text{Wave} \\ \text{type} \\ \text{factor}}}{\Psi_{2j}} \cdot \underset{\substack{\text{Frequency} \\ \text{factor}}}{\Psi_{3j}} \cdot \underset{\substack{\text{Flaw} \\ \text{factor}}}{\Psi_{4j}} \cdot \underset{\substack{\text{Ductile} \\ \text{failure} \\ \text{factor}}}{\Psi_{4j}} \cdot \underset{\substack{\text{Fatigue} \\ \text{failure} \\ \text{factor}}}{\Psi_{5j}} \cdot \underset{\substack{\text{Material} \\ \text{max.} \\ \text{velocity}}}{v_{\max}}$$

FIG. 1. From material property-based maximum particle velocity $v_{\max}$ to case-specific particle velocity limit v_{lim}, via factors Ψ_{1j} to Ψ_{5j} for the jth run using a selected material. Each factor Ψ_{ij} is briefly defined in the text here and detailed later.

181 $v_{\text{lim},j}$ determined above via the following equation:

$$P_{\text{f}}(v) \triangleq \frac{1}{N} \sum_{j=1}^{N} \mathscr{H}\left(v - v_{\text{lim},j}\right), \tag{5}$$

182 where $\mathscr{H}(\chi) \triangleq (\chi + |\chi|)/(2\chi)$ except for $\mathscr{H}(0) \triangleq 1$, the Heaviside step distribution with a

183 dummy variable χ.

184   All this analytical machinery states that, upon choosing a particle velocity v, if $v \geq v_{\text{lim},j}$,

185 the probability of failure for the jth run is 1 or 100%. However, the limiting velocity, $v_{\text{lim},j}$,

186 is different for each (j^{th}) case, because the values of Ψ_{ij} will vary from case to case. Thus

187 under some circumstances the failure may not happen, while others will produce failure. The

188 probability $P_{\text{f}}(v)$ takes all N cases into consideration.

189   We seek to produce a particular order of magnitude estimate for the particle velocity that

190 would lead to a 50% chance of material failure. Given the many possibilities within Ψ_{ij}, this is

191 likely the best we can hope for.

192   We next consider the basic relationship between failure and the maximum particle velocity

193 in a material before considering the details in computing each Ψ_{ij} term required to find the

case-limited particle velocity, v_{lim}. In doing so, we refer to Fig. 2 to illustrate the vibrations and
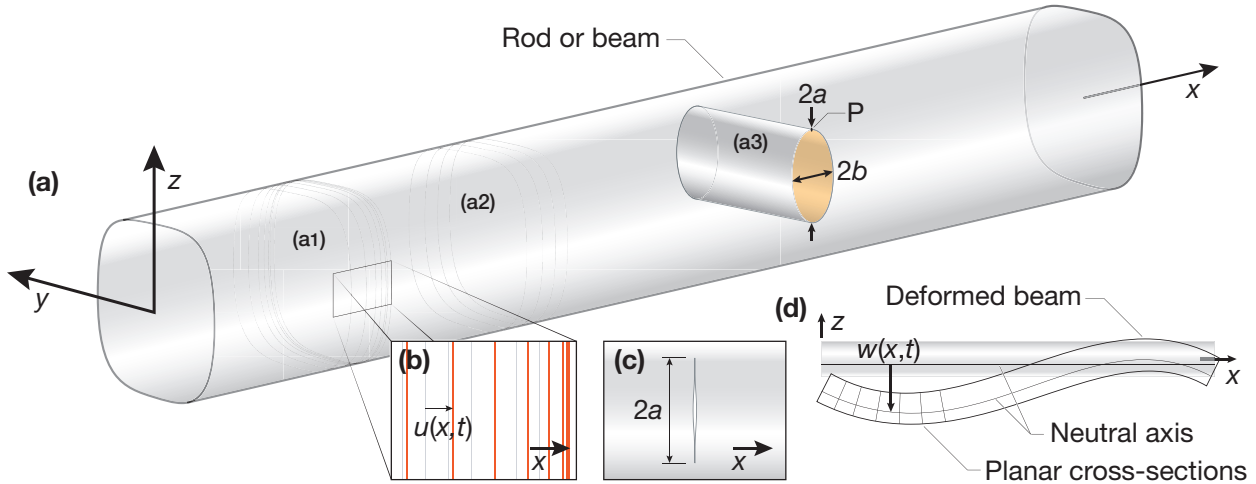
potential flaws.

FIG. 2. A rod or beam made from one of the selected materials may (a) transmit an acoustic longitudinal wave along its length—the x axis. This is seen by a (a1) pattern of (a2) regularly spaced cross-sectional lines becoming (a1,b) closer and farther apart as the acoustic wave progresses along the rod. The (b) motion $u(x,t)$ is a particle displacement along the x axis. There may be lateral contraction along the y and z axes as the acoustic wave stretches the material in the rod along the x axis in a Pochhammer-Chree model of the longitudinal wave propagation, not shown here for clarity. Likewise, shear waves could be present, and instead of $u(x,t)$ along the x axis, there would be lateral motion along either y or z, perhaps both. The stress generated in the rod or a beam could be locally increased due to the presence of a stress concentration, modeled (a3) here as an elliptical flaw penetrating the structure along the y axis. Even if the flaw's edges around its periphery are not sharp, the stress can be significantly greater here, for example at point P, than in the bulk material. Moreover, if the edges are sharp and the material is brittle (with a known K_{IC}), the failure stress may be significantly lower than the yield stress. This is represented in some cases with (c) a through crack of total length $2a$. It is possible that the structure could be transmitting (d) bending instead of axial or shear vibration. We represent this with the Euler-Bernoulli beam model, where the beam is "thin" (over ten times longer than its lateral dimensions), the planar cross-sections remain plane during deformation, the beam is symmetric about the z axis, and the deformation $w(x,t)$ is insufficient to cause significant rotary inertia or shear deformation. This model permits us to define a neutral axis at which the axial stress is always zero.

B. Material Upper Limit Particle Velocity by Yield Stress in One-Dimensional Axial Vibration

We first consider the classic model of one-dimensional planar acoustic waves propagating through a homogeneous media, seeking to set the stage for extensions from this model to produce equally convenient results for other systems.

Internal stress caused by continuous harmonic vibration is a function of material density and stiffness and is proportional to the maximum particle velocity within the solid. That is, the maximum speed a wave moves inside the material can determine the corresponding maximum stress during one full sinusoidal vibration cycle. As previously stated, cyclical plastic deformation—inelastic deformation—during vibration is undesirable and likely limits the particle velocity as well. Thus, we seek a material-dependent maximum particle velocity limit defined by the material-specific yield stress.

An equation that relates the maximum particle velocity during vibration to the material stress may be derived along the lines of Hunt and Crandall's approach and is expressed using the vibrational Mach number ($M_{\mathrm{v}} = V_0/c$)(Crandall, 1962; Hunt, 1960), where V_0 and c are the surface particle velocity amplitude and the acoustic wave phase velocity, respectively. Using linear dynamic elasticity for an isotropic, homogeneous media, the following one-dimensional elastic wave equation may be derived:

$$\frac{\partial^2 u}{\partial x^2} = \frac{1}{c_0^2}\frac{\partial^2 u}{\partial t^2}.$$
(6)

Presuming a harmonic traveling wave of sinusoidal form for displacement $u(x, t)$ produces the solution $u(x, t) = U_0 \sin(\omega t - kx)$ to the wave eqn. (6), with the wavenumber $k = 2\pi/\lambda = \omega/c$.

₂₁₇ Ignoring lateral motion (until later), the strain in a slim rod as this wave propagates along it is

₂₁₈ $\epsilon = \partial u / \partial x$ and the particle velocity is $v = \partial u / \partial t$, producing $\epsilon(x, t) = -v(x, t)/c$. So the maximum

₂₁₉ strain generated by the passage of the acoustic wave in one dimension is

$$\epsilon_{\max} = (V_0/c) = M_{\mathrm{v}}. \tag{7}$$

₂₂₀ The speed of this longitudinal wave is $c = \sqrt{E/\rho}$, where ρ is the material's density and E is its

₂₂₁ Young's modulus. Thus, the maximum stress is,

$$\sigma_{\max} = E\epsilon_{\max} = \sqrt{\rho E} V_0. \tag{8}$$

₂₂₂ We define material failure as equivalent to the condition when the stress at a point in the system

₂₂₃ exceeds the yield stress limit σ_{y} where plastic deformation occurs. Though this is not neces-

₂₂₄ sarily true failure, in the context of continuous vibration it is not desirable since it produces an

₂₂₅ irreversible change in the properties of the system.

₂₂₆ With this definition in mind, the critical particle velocity associated with the material's fail-

₂₂₇ ure due to vibration may be defined as

$$v_{\max} \triangleq \frac{\sigma_{\mathrm{y}}}{\sqrt{\rho E}}. \tag{9}$$

₂₂₈ However, the assumption of a one-dimensional, longitudinally-vibrating, infinite rod in

₂₂₉ Fig. 2 is simply unrealistic for most applications, and so the material property-based particle

₂₃₀ velocity limit in eqn. (9) is inadequate. The geometry, flaws, and size of the vibrating speci-

₂₃₁ men may affect the estimate for this limit (Crandall, 1962; Hunt, 1960). Damping may limit

the maximum possible particle velocity in soft and plastic materials, while imperfections in

brittle materials may cause stress concentrations and a higher risk of fracture-driven failure

(Pritz, 1998). The particle velocity limit also depends on the lateral dimensions of the structure,

sometimes called the "Poisson effect", which can take up elastic energy and effectively act to

slow the speed of sound during vibration (Bancroft, 1941).

C.   Geometric and Acoustic Waveform Effects

In most cases, the vibration under evaluation occurs in complex structures not represented

by simple axial wave propagation theory. The complexity of the structure is likely to signifi-

cantly affect the relationship between particle velocity and material stress. To take this into

account, we consider other forms of vibration and use dimensionless parameters Ψ_{ij} to define

the maximum particle velocity limits for them.

Other modes of vibration may propagate at speeds of sound different than simple longitu-

dinal waves in thin media. For example, shear waves travel at a slower speed: $c_{\text{shear}} = \sqrt{G/\rho} <$

$\sqrt{E/\rho}$. Torsional waves (Liu *et al.*, 2009), Rayleigh waves, flexural waves, or Love waves, among

others, can also propagate in or upon a material.

This affects the relationship between the limiting material stress and the maximum particle

velocity. For example, flexural waves in beams propagate far slower than longitudinal waves,

implying the maximum particle velocity is greater for flexural waves. But there is more to con-

sider. In modeling flexural waves in beams, for example, the Timoshenko beam model includes

the effects of rotational inertia and lateral shearing ignored in the Euler-Bernoulli beam model,

leading to an even slower wave speed in a Timoshenko beam and consequently a greater maxi-

mum particle velocity at failure (Hunt, 1960). Changing a model can change the estimate of the maximum particle velocity. The many models devised over the years for beams, membranes, rods, plates, shells, and other structures and the details they demand could easily overwhelm any effort to find a ubiquitous maximum particle velocity, if it exists.

Our approach to this problem is the observation that while these different models are certainly important, they do not affect the relationship between the limiting material stress and the maximum particle velocity beyond about an order of magnitude. Since we *seek to only find the order of magnitude of the maximum particle velocity*, we may choose a representative subset of the models to proceed. While it may be true that including more models of other phenomena would improve our estimate, we contend it is unlikely to significantly change the results. And even then, our aim here is to demonstrate a process for finding the maximum particle velocity across a series of models using a statistical approach, which we believe to be useful for design choices and developing an intuitive feel for what limits the propagation of acoustics and vibrations in materials and structures.

We can furthermore expect that whatever form the vibration might be, in an elastic media the basic relation between the maximum particle velocity and the limiting stress will be analogous to the relation found for longitudinal vibrations, differing only by a constant (Hunt, 1960). Evidence of this is provided in a broader derivation in the Appendix. In lieu of considering every possible form of vibration, we next consider a pair of simple cases: transverse vibration of a beam and axial wave propagation in a narrow rod.

1. Transverse vibration of an Euler-Bernoulli beam

To illustrate our point in a concrete manner, we first consider the Euler-Bernoulli beam model for transverse, flexural vibration of a beam, and then return to axial vibration with the Pochhammer-Chree rod model. The Euler-Bernoulli beam equation, for a homogeneous elastic and slender beam, is

$$-EI\frac{\partial^4 w}{\partial x^4} = \rho A\frac{\partial^2 w}{\partial t^2}, \tag{10}$$

where I, A, and $w(x,t)$ are the second moment of area of the beam's cross-section, the area of the beam's cross-section, and transverse displacement shown in Fig. 2(d), respectively, with the displacement dependent upon the axial coordinate x and time t. The corresponding stress is $\sigma(x,y,t) = EI\frac{\partial^2 w}{\partial x^2}$ at any point in the beam. The maximum stress, $\sigma_{\max}$, is located at $y_{\max} = Y$, the maximum distance from the neutral axis along the cross-section of the beam, and is given by

$$\sigma_{\max} = k\sqrt{E\rho}\, v, \tag{11}$$

with $k = \sqrt{EA/I}$ as a factor dependent upon the cross-sectional shape. Since typical beams have a convex cross-sectional shape, this factor, k, is typically greater than one, and may be as small as $k = \sqrt{3}$ for a rectangular cross-section and as large as $k = 2\sqrt{2}$ for a triangular cross-section. We choose to represent k in our modeling as a normally (Gaussian) distributed random value between these two limiting cases. The justification for a normal distribution, instead of, say, a uniform distribution is the observation that these limiting beam shapes are less common than those that produce intermediate values of k. In any case, the net effect upon the results of choosing another distribution for this factor is minor.

18

²⁹² The maximum particle velocity limit is *reduced* from the longitudinal wave-based prediction

²⁹³ in eqn. (9) by a factor of $1/k$. In other words, the limiting particle velocity limit due to the

²⁹⁴ transverse vibration of an Euler-Bernoulli beam is $v_{\text{lim}} = \Psi_{1j} v_{\text{max}}$, where $\Psi_{1j} = 1/k_j$ and k_j is a

²⁹⁵ uniformly random value between $\sqrt{3}$ and $2\sqrt{2}$.

2. Axial wave propagation in a rod and the Pochhammer-Chree solution

²⁹⁷ Returning briefly to longitudinal wave vibration, one potential geometric effect that may ap-

²⁹⁸ pear is the lateral confinement and elasticity ignored by the one-dimensional analysis. This is

²⁹⁹ known to introduce an additional degree of freedom to an acoustic wave propagating through

³⁰⁰ the structure. The motion will reduce the speed of sound for the propagation of the wave, lead-

³⁰¹ ing to a change in the relation between the terms in eqn. (7) and consequently eqn. (9). We

³⁰² consider a simple elastic, homogeneous, and isotropic round bar with circular cross section as

³⁰³ a representative example of this phenomena. As the diameter of the rod, $D \to \infty$, this effect

³⁰⁴ would likewise become negligible, returning us to the original model in subsection II B. How-

³⁰⁵ ever, for small values of $D < 2\lambda$, the actual speed of sound c_{rod} is reduced as either the Poisson's

³⁰⁶ ratio ν or the diameter-to-wavelength ratio $\Delta = D/\lambda$ is increased (Bancroft, 1941). Thus, based

³⁰⁷ on eqn. (9), the limiting particle velocity for a longitudinal wave including lateral effects would

³⁰⁸ be $v_{\text{lim},j} = \Psi_{1j} v_{\text{max}}$, where $\Psi_{1j} = c_{\text{rod},j}/c_0$. The index j refers to the jth run using a particular

³⁰⁹ material in the analysis, where $c_{\text{rod},j}/c_0$ is chosen at random with uniform distribution over the

³¹⁰ range 0.563 to 1 based on physically permissible values of Poisson's ratio, ν, and the diameter-

³¹¹ to-wavelength ratio $\Delta = D/\lambda$ according to Bancroft (1941).

19

₃₁₂ **D.   The Effects of the Frequency of the Acoustic Wave on Damping and Dynamic Material Stiffness**

₃₁₃ Since the Young's modulus of an isotropic material under vibration actually depends upon

₃₁₄ the frequency of the vibration (Pritz, 1998), significantly stiffening with an increase in the fre-

₃₁₅ quency, the ratio of Young's modulus appropriate for this frequency, the *dynamic* Young's mod-

₃₁₆ ulus $E(f)$, to its (nearly) static counterpart, E_0, may be approximated from the loss factor,

$$\eta = \frac{\pi}{2} \frac{\log(\frac{E(f)}{E_0})}{\log(\frac{f}{f_0})},\tag{12}$$

₃₁₇ where we suppose $f_0 = 1$ Hz, $E_0 \sim E(f_0)$ represents low-frequency vibration (Pritz, 1998). There-

₃₁₈ fore, we may define the reduction in the limiting particle velocity due to damping and the fre-

₃₁₉ quency of the acoustic wave as

$$\Psi_{2j} = \sqrt{\frac{E_0}{E(f_j)}} = \left(10^{-\frac{2\eta}{\pi}}\right) \frac{f_0}{f_j}.\tag{13}$$

₃₂₀ Later, when we use eqn. (13) to statistically determine the limiting particle velocity by produc-

₃₂₁ ing N total runs for each material, the frequency f_j as a random value between 10^0 Hz and

₃₂₂ 10^9 Hz on a base-ten logarithmic scale, a typical range for the majority of acoustic phenomena.

₃₂₃ **E.   Effects of Flaws as Stress Concentrations and Cracks**

₃₂₄ Flaws in most engineering materials can significantly reduce the failure stress. Depending

₃₂₅ on the orientation and size of the flaw, a stress concentration may locally form around the

₃₂₆ flaw and contribute to broader failure of the material. It is overwhelmingly difficult to pursue

₃₂₇ broad treatment of elastoplastic fracture mechanics applied to the many forms of stress and

20

flaw shapes that may arise in practical situations. Moreover, the micromechanics of failure in flawed media is a complex subject under study for many years (Curran *et al.*, 1987). Instead of being drawn into these aspects, we once again choose an exemplar to represent an order-of-magnitude estimate of this phenomena: elliptical flaws in a material, uniaxially loaded by stress, σ, as the vibration or acoustic wave propagates through the system, producing a large range of stress concentration factors due to variance in their size and orientation. If the material is also brittle, then the material may separately fail by exceeding its critical fracture toughness as the flaw becomes sharp-tipped: a crack.

1.   Ductile failure

Stress concentrations in a ductile material around a flaw may produce plastic yielding that represents failure as an acoustic wave is transmitted through it. For example (Anderson and Anderson, 2005), in an elliptical through flaw of length $2a$ by $2b$, the stress produced near the flaw's semimajor axis end (*see* point P in Fig. 2(a3)), σ_c, is greater than the uniaxial stress σ_y by a factor ϕ representing the stress concentration. Here, $2a$ is oriented along z and $2b$ is oriented along x; the flaw extends all the way through the structure along y. For this flaw geometry, illustrated in Fig. 2(a3), $\sigma_\mathrm{c} = \phi\sigma_\mathrm{y}$, where $\phi = 1 + 2(a/b)$. This implies that once $\sigma_\mathrm{c} \rightarrow \sigma_\mathrm{f}$, the failure stress or $\sigma_\mathrm{c} \rightarrow \sigma_\mathrm{y}$, the yield stress, the result is at least local plastic yielding that would be undesirable in continued vibration. At worst, the material fails. With this potential flaw representing the class of myriad flaws that may be present in ductile materials, the limiting particle velocity will be the maximum particle velocity scaled by the factor $\Psi_{3j}^{-1} \triangleq \phi_j = 1 +$

348 $2(a_j/b_j)$. For our statistical analysis, we require the ratio (a_j/b_j) to be randomized between 0.1

349 to 10 on a base-ten logarithmic scale.

2. Brittle failure

351 In a brittle material, the stress in the vicinity of a sharp-tipped crack is generally dependent

352 on the square root of the distance from the crack tip, and it and the growth of the crack to

353 eventual failure both depend upon the *fracture toughness* K_C, a material property. The *stress*

354 *intensity factor, K*, may be calculated for a given stress and crack size, and here we choose as

355 our exemplar the plane strain mode I fracture toughness, K_{IC}. As a defined property of brittle

356 materials, it may be used to determine the failure stress, $\sigma_f = K_{IC}/\sqrt{a\pi}$, for a crack of length $2a$

357 centrally located in a thin, semi-infinite plate material. The crack is presumed to be perpendic-

358 ularly oriented to the direction of the stress as shown in Fig. 2(c).

3. Failure in flawed material for a given analysis is either due to brittle or ductile failure

360 The randomly preselected crack size for each run is a_{sj}, randomly defined between 10^{-6}

361 and 1 mm on a base-ten logarithmic scale. Depending on this crack length, some materials

362 may either fail via brittle or ductile failure. To determine which, we determine the critical crack

363 size for brittle failure,

$$a_c = \frac{1}{\pi}\left(\frac{K}{\sigma_y}\right)^2,\tag{14}$$

364 where σ_y is the yield stress. For the jth run, if $a_{sj} > a_c$, the material will fail from the brittle

365 crack, and the limiting particle velocity is further reduced due to this by a factor $\Psi_{4j} = \sqrt{\frac{a_c}{a_{sj}}}$. If,

22

however, $a_{sj} < a_c$, the material will fail by exceeding the ductile yield stress, σ_y, before brittle failure becomes a problem, and so $\Psi_{4j} = 1$.

F.   Effects of Endurance and Fatigue

Ductile materials may also fail under cyclical stresses well below the material's yield stress. Cyclical vibrations from acoustic wave transmission and vibration, in particular, may exceed a material's endurance limits due to fatigue that accumulates with time. As with the other effects, the many ways this effect may impact a given material's response to vibration depends upon the characteristics of the material and the vibration, and so we again constrain our analysis into a tractable version by limiting the number of vibration cycles to at most 10^6 and a frequency between 0.1 kHz to 1 MHz on a base-ten logarithmic scale when fatigue is relevant. Fatigue arises in the context of structural vibration and in this context is only relevant over this limited frequency range. The fatigue endurance-limited stress of such a material after 10^6 cycles is written as σ_E, and is less than the yield stress σ_y. We define in the statistical analysis the effect this would have on the limiting particle velocity as $\Psi_{5j} \triangleq \sigma_E/\sigma_y$.

III.   RESULTS

The probability of failure of eleven selected materials—diamond, steel, aluminum, copper, polypropylene (PP), polyvinyl chloride (PVC), Polymethyl methacrylate (PMMA), glass, concrete, wood, and lithium niobate—illustrates a consistent trend towards failure at a particle velocity of $v = \mathcal{O}[0.1 - 10]$ m/s (Fig. 3). The results produced by $N = 10,000$ runs per material is monotonically increasing with respect to the particle velocity in the plot, with the horizontal

23
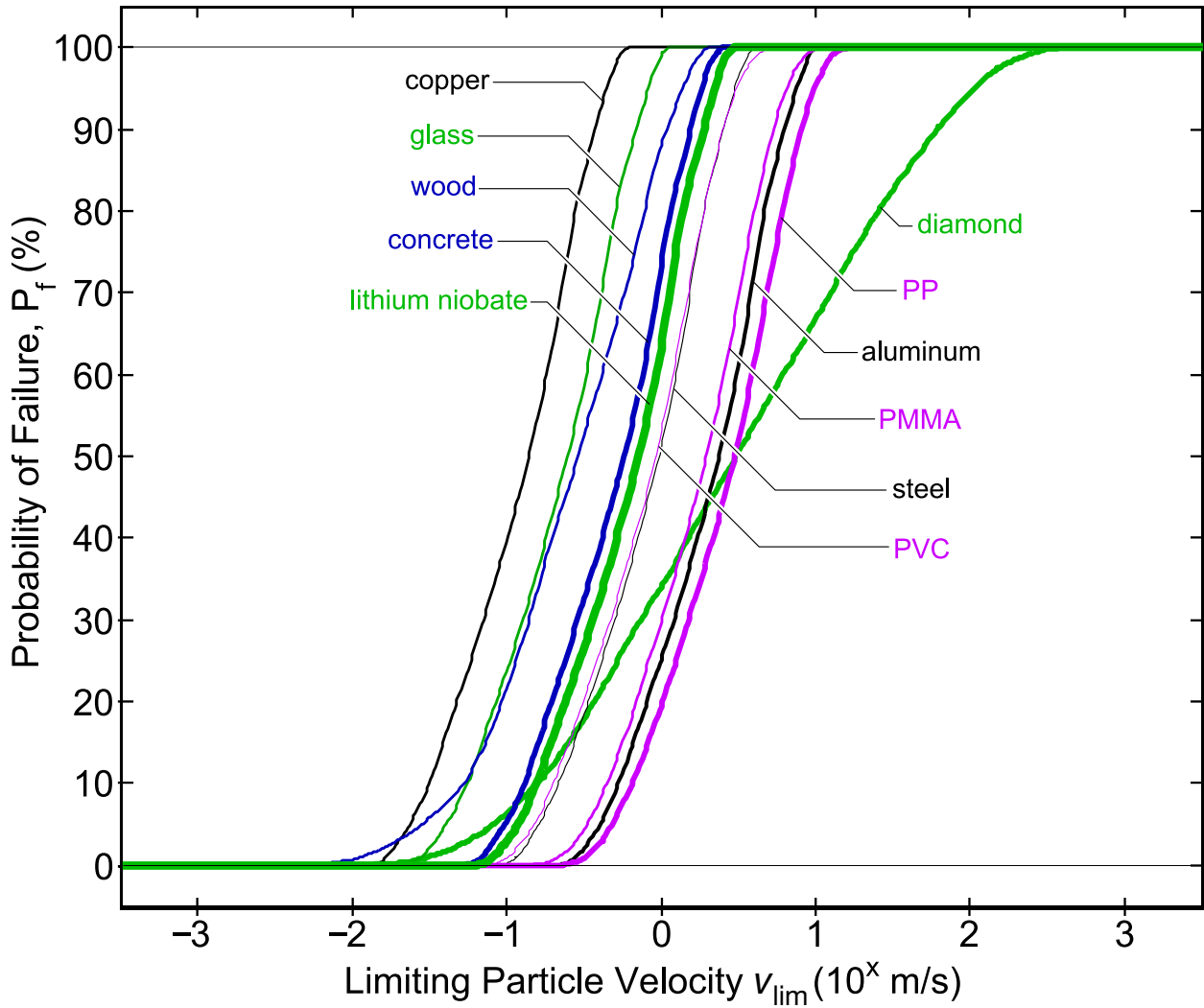
FIG. 3. The probability of failure P_f versus particle velocity v for eleven selected materials (*see* text). Ten thousand (N) runs for each material choice produces a nearly continuous distribution of failure probability with respect to the particle velocity. The result is nearly sigmoidal, but with small yet important discrepancies between materials and over v. These arise from the effects of the different forms of acoustically-driven failure.

axis plotted as a base-ten logarithm for clarity. There is no scatter in this data nor error bars to provide as each (j^{th}) result lies at a specific combination of the particle velocity and probability of failure.

We then nondimensionalize the particle velocity as $\hat{v} \triangleq v/v_{\max}$, remembering that $v_{\max}$ is a material property. By further considering the probability of failure based on this dimensionless particle velocity $v/v_{\max}$, the data appears to collapse to produce a similar probability of failure for a given dimensionless particle velocity $\hat{v}$ regardless of the chosen material in Fig. 4, with the notable exceptions of diamond and wood. These two examples indicate the importance of the toughness of flawless diamond, the fragility of diamond with flaws, and the unique failure characteristics of wood. Wood has extremely large yield and failure stress values when considering its other properties, due to its composite and porous structure, and this strongly affects the predicted results despite the absence of anisotropy. Other single crystal and composite media are likely to exhibit similar results.

Referring to the results in Figs. 3 and 4, the probability of failure at low vibration velocities with $P_{\mathrm{f}} \approx 0$ until 10^{-2} m/s, where wood, copper, diamond, and glass are first to exhibit nonzero failure probabilities, followed by steel, lithium niobate, aluminum, and the polymers. Diamond produces a different distribution of failure probabilities with respect to particle velocity than the other materials, partially a consequence of its hardness and high yield stress, and partially because it is more fragile than most of the other materials when it has a flaw.

Crucially, consider the distribution of particle velocities at which $P_{\mathrm{f}} = 50\%$ for the chosen materials, as tabulated in Table I. The results indicate that the mean particle velocity at $P_{\mathrm{f}} = 50\%$ is 1.31 m/s for these eleven materials, incorporating various forms of vibration, frequencies, flaws, and fatigue. With the 95% confidence interval from 0.46 to 1.58 m/s ($10^{-0.07\pm0.27}$ m/s) for v_{lim} predicted from logistic regression of all the data for all materials, it appears reasonable to conclude that a limiting particle velocity of $v_{\mathrm{lim}} = \mathcal{O}[1 \text{ m/s}]$ exists. Furthermore, by non-
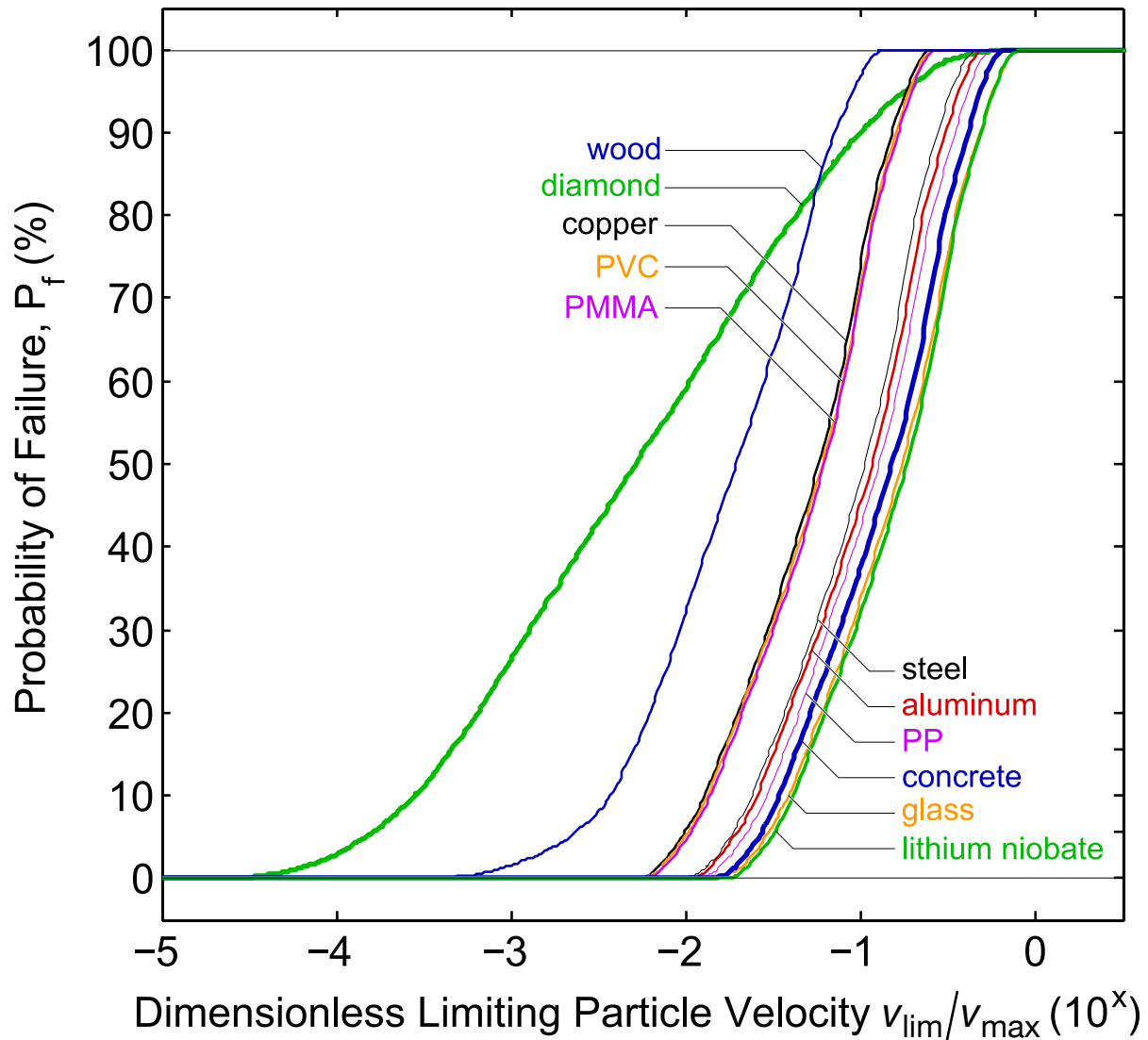
25

FIG. 4. Probability of failure P_f versus the dimensionless particle velocity $\hat{v}$ for the eleven selected materials. Diamond exhibits a broader range of particle velocities over which failure may occur because of its unique toughness without flaws and fragility with flaws. Most of the other materials, except for wood, fall into a narrowly defined group.

412   dimensionalizing the data, a dimensionless limiting particle velocity also may be predicted to

413   be $\hat{v}_{lim} = \mathcal{O}[0.1]$ with a 95% confidence interval within 0.034 to 0.12 ($10^{-1.19\pm0.28}$) via logistic

414   regression.

TABLE I. Particle velocity, dimensional (v) and dimensionless ($\hat{v}$), for each of the selected materials where the probability of failure at $P_\text{f} = 50\%$ over all $N = 10000$ cases per material.

Material	v (m/s)	$\hat{v}$ (—)
Copper	0.14	0.06
Glass	0.25	0.18
Wood	0.30	0.02
Concrete	0.58	0.15
Steel	0.96	0.11
Polyvinyl Chloride (PVC)	0.93	0.04
Aluminum	2.40	0.12
Acrylic (PMMA)	2.04	0.05
Diamond	3.09	0.005
Polypropylene (PP)	3.02	0.10
Lithium Niobate (LN)	0.69	0.19
Mean	1.31	0.09
95% Confidence Interval	0.46 – 1.58	0.034 – 0.12

IV. APPLICATION TO ACOUSTOFLUIDICS

Surface acoustic waves (SAW) are both classic and modern, with wide use in communications since the classic development of interdigital transducer (IDT) electrodes in 1965 (White and Voltmer, 1965) and numerous acoustofluidics applications in the past twenty years (Connacher *et al.*, 2018a; Friend and Yeo, 2011). Only in acoustofluidics has it become necessary to drive the devices near their structural limits, leading to rapid device failure. The maximum particle velocity on the substrate has been empirically shown to be $\mathcal{O}[1 \text{ m/s}]$ (Friend and Yeo,

[422] [2011](), but there has been no theoretical analysis nor experimental results to show why this actually occurs or might be important. Here, we present the surface particle velocity amplitude on a lithium niobate (LN) substrate due to IDT-generated SAW. The velocity is measured via laser Doppler vibrometer, exhibiting a maximum particle velocity of $\mathcal{O}[1 \text{ m/s}]$.

A.   Experimental Setup and Results for Surface Acoustic Wave Particle Velocity Measurement

[427] We designed and fabricated SAW interdigital transducer (IDT) devices on double-side polished 128° Y-rotated cut LN (Precision Micro-Optics Inc., Burlington, MA,USA) for surface acoustic wave generation and propagation. The fabrication and usage details, including images of the devices, are provided in ample detail elsewhere (Mei *et al.*, 2020). A wavelength of $\lambda = 100\ \mu$m was selected for an operating frequency of ~40 MHz (from $f = \nu/\lambda$) to define each IDT, comprised of twenty simple finger pairs with finger and gap widths of $\lambda/4$ and an aperture of 2 mm. For lithium niobate wafers of 500 μm thickness, 40 MHz is approximately the minimum frequency that may be used to generate useful Rayleigh SAW. Lower frequencies typically reported in much of the acoustofluidics literature are actually generating Lamb waves instead (Connacher *et al.*, 2018b). Standard UV photolithography (using AZ 1512 photoresist and AZ 300MIF developer, MicroChem, Westborough, MA) was used alongside sputter deposition and lift-off processes to fabricate the 10 nm Cr / 1 μm Au IDT upon the 500 μm thick LN substrate (Connacher *et al.*, 2018b). Absorbers (Dragon Skin™, Smooth-On, Inc., Macungie, PA) were used at the center and periphery of the device to prevent edge reflections and spurious bulk waves. Surface acoustic waves were generated by applying a sinusoidal electric field to the IDT at resonance using a signal generator (WF1967 multifunction generator, NF Corporation,

28

Yokohama, Japan) and amplifier (ZHL–1–2W–S+, Mini-Circuits, Brooklyn, NY, USA). The actual voltage, current, and power across the device were measured using an oscilloscope (InfiniVision 2000 X-Series, Keysight Technologies, Santa Rosa, CA). The particle velocity perpendicular to the substrate surface was measured using a laser Doppler vibrometer (LDV, UHF–120SV, Polytec, Waldbronn, Germany).

By increasing the voltage of the signal delivered to the IDTs, the particle velocity of the SAW perpendicular to the substrate surface also increases—to a limit. The particle velocity increases linearly when the voltage is relatively small, up to an apparent limit at about 1.2 to 1.4 m/s; this limit at $\mathscr{O}[1]$ m/s appears when the input signal is relatively large, and remains relatively constant until the device fails in this example at around 20 V. When using these devices, the brittle LN can unexpectedly and suddenly fail once the vibration velocity reaches $\mathscr{O}[1]$ m/s; by contrast, using such devices at lower vibration velocity amplitudes is possible for months to years.

This device is a simple version of the many such devices used for acoustofluidics. The SAW is converted into sound propagating in a fluid in contact with such a substrate. Because this sound is intense and produces compressibility in the fluid, a combination of the density variations and particle velocity—in the presence of viscosity sufficient to cause a phase shift between them—altogether gives rise to acoustic streaming. Acoustic streaming is transmitted most often via the streamwise acceleration or the Reynolds stress, and scales with ρU^2, where ρ and U are the fluid density and amplitude of the LN surface's particle velocity, respectively. Since $U \sim 1$ m/s for the LN substrate at its limit, the steady acoustic pressure is ~ 1 kPa for most fluids. This is a relatively weak pressure limit and is difficult to improve upon, a key reason why
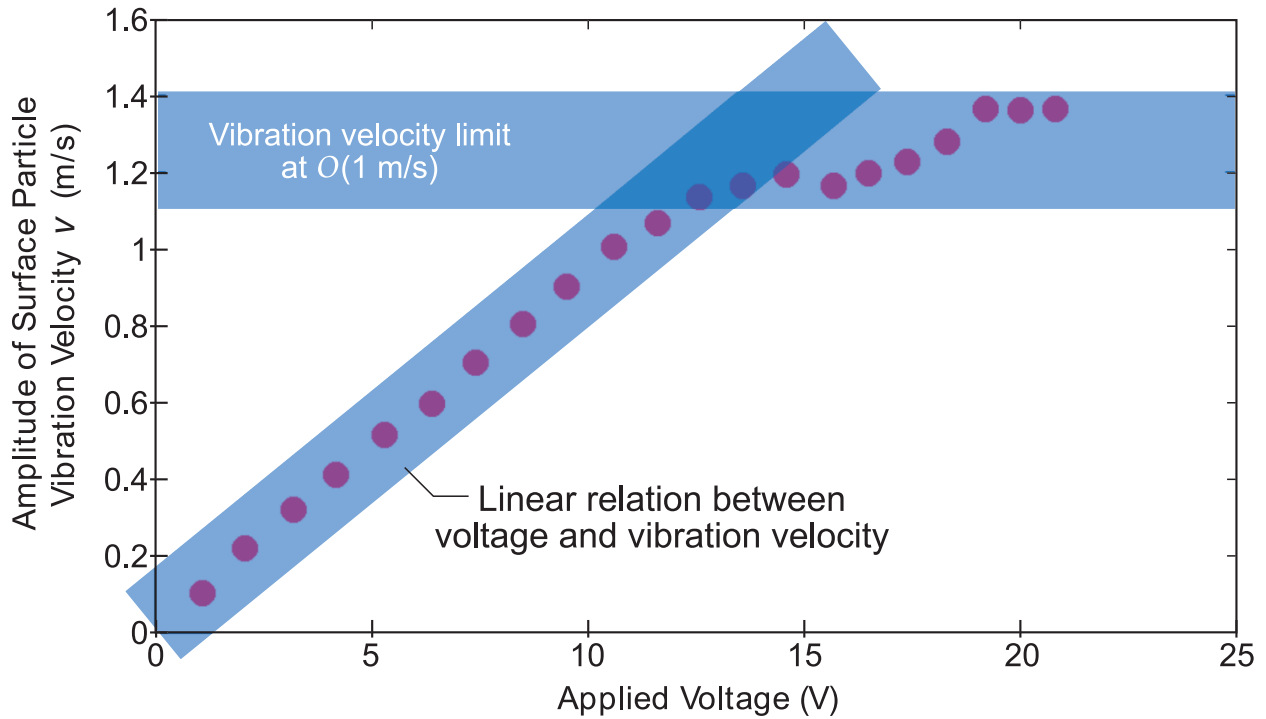
29

FIG. 5. Particle velocity of SAW generated and propagating upon a lithium niobate substrate versus the applied voltage on the IDT. There is a linear relation between an increasing applied voltage and the particle velocity, until 15 V, at which point the particle velocity becomes essentially constant between 1.2 and 1.4 m/s, corresponding to the estimated particle velocity limit of $\mathcal{O}[1 \text{ m/s}]$ from the earlier analysis.

acoustic streaming in its traditional form is not very effective in high-pressure applications. However, there are other approaches that may produce useful results (Zhang *et al.*, 2021a,b), exploiting alternatives to acoustic streaming by relying on the nonlinear coupling between an enclosing channel's deformation and the propagation of the primary sound field in the fluid to produce far greater pressures and flow speeds. The key point is that while there are many advantages to using acoustic waves in propelling fluids via acoustic streaming, seeking to do so against anything more than a modest pressure head is unlikely to work.

V. CONCLUSIONS

We have sought to define a limiting particle velocity for acoustic waves and vibrations as defined upon the concept of material failure in a variety of conditions and material choices. The relationship between maximum particle velocity and maximum stress during vibration has been found and used for this purpose. While the particle velocity limit is not merely defined by material failure, it can be treated in this way by noting that the appearance of inelastic material responses—plasticity, significant anelastic damping—may be included as "failure" in the context of acoustic waves and vibrations because these phenomena will limit the particle velocity all the same.

The particle velocity limits were defined in terms of the maximum particle velocity, a material property. Dimensionless parameters Ψ_{ij} were defined to represent geometric effects and modes of vibration, damping, cracks and imperfections, endurance and fatigue, and the weakening of the material due to cracks in brittle materials. Statistical results were presented using the Monte Carlo method for eleven different materials of $N = 10000$ specimens each, randomizing the geometry, wave modes, and frequency to relate the probability of material failure to the limiting particle velocity. A limiting particle velocity of $v_{\text{lim}} = \mathcal{O}[1 \text{ m/s}]$ exists with a 95% confidence interval from 0.46 to 1.58 m/s ($10^{-0.07 \pm 0.27}$ m/s) predicted from logistic regression of all the data for all materials, types of vibration, and failure modes considered in this study. The nondimensional limit is $\hat{v}_{\text{lim}} = \mathcal{O}[0.1]$ with a 95% confidence interval from 0.034 to 0.12.

The concept of the limiting particle velocity as an invariant at $\mathcal{O}[1 \text{ m/s}]$ is useful when one recognizes that the classic use of acceleration as a failure criteria does not apply in acoustic

31

devices. Acceleration is not invariant with respect to frequency. Similarly, the displacement amplitude cannot be used because it is likewise dependent upon the frequency. Regardless of the phenomenon and its frequency, one may begin with the assumption that failure of a material may be a risk when $\mathscr{O}[1 \text{ m/s}]$. Beyond failure, anelastic response of materials may equally arise at this particle velocity, suggesting it as a practical limit to motion that may be induced in a material without extraordinary effort or damaging the material's integrity. In other words, even if the material does not fail, it may fail to produce larger amplitude responses due to energy losses. This was illustrated via a simple experiment where SAW was generated across the surface of lithium niobate.

The consequences of particle velocity limit analysis can effectively be used in materials and structural engineering to predict when dynamic material vibration velocity can cause failure in various forms (i.e., brittle fracture, repeated plastic deformation, fatigue failure). Furthermore, this analysis may be useful in predicting the potential amplitude and frequency limits of actuators that rely on resonant or driven vibrations. In the future, material structures evaluated for vibration failure via finite element modeling of complex geometry, damping, and flaws may be simplified. Rather than calculating the likelihood of dynamic failure by localized time-dependent stress-strain relationships, strain energy expressions, or bespoke failure models, the local nodal velocity could be used as a proxy for predicting failure and the presence of damaging vibrations.

Finally, the implications of $\mathscr{O}[1 \text{ m/s}]$ as a limiting particle velocity are profound when exploring the highest end of the frequency range $f = 1$ Hz to 1 GHz that we considered. With $v_{\text{lim}} = \mathscr{O}[1 \text{ m/s}]$, we have a maximum displacement of only $u_{\text{lim}} = (2\pi f)^{-1} v_{\text{lim}} \mathscr{O}[0.1 \text{ nm}]$ at

32

1 GHz, yet an acceleration of $\alpha_{\lim} = 2\pi f \, v_{\lim} \mathcal{O}[10^{10}]$ m/s^2. Such large accelerations are responsible for many of the peculiar phenomena observed and reported in acoustofluidics, and will surely be the source of more interesting results to come.

ACKNOWLEDGMENTS

REFERENCES

Anderson, T., and Anderson, T. (**2005**). *Fracture Mechanics: Fundamentals and Applications, Third Edition* (Taylor & Francis, Philadelphia, PA USA), https://books.google.com/books?id=MxrtsC-ZooQC.

Auld, B. (**1990**). number v. 1 in Acoustic Fields and Waves in Solids *Acoustic Fields and Waves in Solids* (R.E. Krieger, Melbourne, FL USA).

Bachmann, P. (**1894**). *Die analytische zahlentheorie*, **2** (Teubner).

Bancroft, D. (**1941**). "The velocity of longitudinal waves in cylindrical bars," Physical Review **59**(7), 588.

Carfagni, M., Lenzi, E., and Pierini, M. (**1998**). "The loss factor as a measure of mechanical damping," in *SPIE proceedings series*, pp. 580–584.

Collins, L. (**2004**). "Picoplatters," IEE Review **50**(4), 44–47.

Connacher, W., Zhang, N., Huang, A., Mei, J., Zhang, S., Gopesh, T., and Friend, J. (**2018**a). "Micro/nano acoustofluidics: materials, phenomena, design, devices, and applications," Lab on a Chip **18**, 1952–1996.

Connacher, W., Zhang, N., Huang, A., Mei, J., Zhang, S., Gopesh, T., and Friend, J. (**2018**b). "Micro/nano acoustofluidics: materials, phenomena, design, devices, and applications," Lab on a Chip **18**(14), 1952–1996.

Cosenza, E., and Manfredi, G. (**2000**). "Damage indices and damage measures," Progress in Structural Engineering and Materials **2**(1), 50–59.

Crandall, S. H. (**1962**). "Relation between strain and velocity in resonant vibration," The Journal of the Acoustical Society of America **34**(12), 1960–1961.

Curran, D., Seaman, L., and Shockey, D. (**1987**). "Dynamic failure of solids," Physics Reports **147**(5), 253 – 388.

Dehghani, H., and Ataee-Pour, M. (**2011**). "Development of a model to predict peak particle velocity in a blasting operation," International Journal of Rock Mechanics and Mining Sciences

$_{556}$ **48**(1), 51–58.

$_{557}$ Demirbas, A. (**2007**). "Fuel alternatives to gasoline," Energy Sources, Part B: Economics, Plan-

$_{558}$ ning, and Policy **2**(3), 311–320.

$_{559}$ Friend, J. R., and Yeo, L. Y. (**2011**). "Microscale acoustofluidics: Microfluidics driven via acous-

$_{560}$ tics and ultrasonics," Reviews of Modern Physics **83**, 647–704.

$_{561}$ Gaberson, H., Pal, D., and Chapler, R. (**2000**). "Shock spectrum classification of violent environ-

$_{562}$ ments that cause machinery failure," in *Proceedings of the 18th International Modal Analysis*

$_{563}$ *Conference*, pp. 1126–1135.

$_{564}$ Halfpenny, A. (**1999**). "A frequency domain approach for fatigue life estimation from finite ele-

$_{565}$ ment analysis," in *Key Engineering Materials*, Trans Tech Publ, Vol. 167, pp. 401–410.

$_{566}$ Hancock, J., and Bommer, J. J. (**2006**). "A state-of-knowledge review of the influence of strong-

$_{567}$ motion duration on structural damage," Earthquake Spectra **22**(3), 827–845.

$_{568}$ Hunt, F. V. (**1960**). "Stress and strain limits on the attainable velocity in mechanical vibration,"

$_{569}$ The Journal of the Acoustical Society of America **32**(9), 1123–1128.

$_{570}$ Kimberley, J., Cooney, R., Lambros, J., Chasiotis, I., and Barker, N. (**2009**). "Failure of au RF-

$_{571}$ MEMS switches subjected to dynamic loading," Sensors and Actuators A: Physical **154**(1), 140

$_{572}$ – 148.

$_{573}$ Liu, D. K.-C., Friend, J., and Yeo, L. (**2009**). "The axial-torsional vibration of pretwisted beams,"

$_{574}$ Journal of Sound and Vibration **321**(1-2), 115–136.

$_{575}$ Mei, J., Zhang, N., and Friend, J. (**2020**). "Fabrication of surface acoustic wave devices on

$_{576}$ lithium niobate," JoVE (Journal of Visualized Experiments) (160), e61013.

577 Mikitarenko, M., and Perelmuter, A. (**1998**). "Safe fatigue life of steel towers under the action of

578 wind vibrations," Journal of Wind Engineering and Industrial Aerodynamics **74**, 1091–1100.

579 Nwosu, H., Obieke, C., and Ameh, A. (**2016**). "Failure analysis and shock protection of external

580 hard disk drive," Nigerian Journal of Technology **35**(4), 855–865.

581 Pritz, T. (**1998**). "Frequency dependences of complex moduli and complex poisson's ratio of

582 real solid materials," Journal of Sound and Vibration **214**(1), 83–104.

583 Ramesh, K., Hogan, J. D., Kimberley, J., and Stickle, A. (**2015**). "A review of mechanisms and

584 models for dynamic failure, strength, and fragmentation," Planetary and Space Science **107**,

585 10 – 23.

586 Standard, M. (**1989**). "Environmental test methods and engineering guidelines," MILSTD-810E,

587 AMSC F **4766**.

588 Watson, B., Friend, J., and Yeo, L. (**2009**). "Piezoelectric ultrasonic micro/milli-scale actuators,"

589 Sensors and Actuators A: Physical **152**, 219–233.

590 White, R. M., and Voltmer, F. W. (**1965**). "Direct piezoelectric coupling to surface elastic waves,"

591 Applied Physics Letters **7**(12), 314–316.

592 Zhang, N., Horesh, A., and Friend, J. (**2021**a). "Manipulation and mixing of 200 femtoliter

593 droplets in nanofluidic channels using mhz-order surface acoustic waves," Advanced Science

594 (Accepted 12 March 2021).

595 Zhang, N., Horesh, A., Manor, O., and Friend, J. (**2021**b). "Powerful acoustogeometric streaming

596 from dynamic geometric nonlinearity," Physical Review Letters (Accepted 19 March 2021).

597 Zhang, Q. B., and Zhao, J. (**2014**). "A review of dynamic experimental techniques and mechan-

598 ical behaviour of rock materials," Rock Mechanics and Rock Engineering **47**(4), 1411–1478.

Appendix

1. Key Parameters and Notations

Parameter	Notation	SI Units
"Defined as"	$\triangleq$	—
Acceleration	α	m/s
Crack size	a	m
Critical crack size	a_c	m
Cross section area	A	m^2
Sound velocity in solid, longitudinal, one dimensional	c_0	m/s
Sound velocity in solid, longitudinal, circular rod	c_rod	m/s
Circular rod diameter	D	m
Young's modulus	E	Pa
Frequency of vibration	f	Hz
Ductility factor	F_duct	m
Shear modulus	G	Pa
Second moment of area	I	m^4
Fracture toughness	K_IC	$\text{Pa}\sqrt{\text{m}}$
Wavelength in solid	λ	m
Poisson's ratio	μ	—
Vibrational Mach number	M_v	—
Number of cases per material	N	—
Order of approximation error (Bachmann, 1894)	$\mathscr{O}$	<varies>
Probability of failure	P_f	%
Factor reducing maximum particle velocity to produce limiting particle velocity	Ψ_{ij}	—
Density	ρ	kg/m^3
Stress	σ	Pa
Endurance limit	σ_E	Pa
Brittle fracture failure stress	σ_f	Pa
Yield strength	σ_y	Pa
Time	t	sec
Longitudinal displacement	u(x,t)	m
Vibration velocity	ν	m/s
Limiting vibration velocity	ν_lim	m/s
Maximum vibration velocity	ν_max	m/s
Circular frequency	ω	rad/s
Transverse displacement	w(x,t)	m
Distance to neutral axis (bending)	y	m

2. A Derivation of the Relationship Between the Maximum Particle Velocity and the Stress for a Planar Acoustic Wave in an Elastic Medium

a. Introduction

The purpose of this appendix is to illustrate to readers the general applicability of the concept relating the particle velocity to the strain, and consequently the material properties. We progress through a brief derivation of the governing equations and a simple solution of them for an isotropic material. Solutions for anisotropic materials, coupled media, and finite deformations build upon this basic approach, though often demand computation to produce solutions.

b. The equation of motion for a solid elastic material

Derivation of Newton's second law for an infinitesimal volume of elastic media (Auld, 1990) produces

$$\nabla \cdot \mathbf{T} + \mathbf{f} = \rho \frac{\partial^2 \mathbf{u}}{\partial t^2}, \tag{15}$$

and, in component notation, we are able to write

$$\frac{\partial T_{ik}}{\partial x_k} + f_i = \rho \frac{\partial^2 u_i}{\partial t^2}. \tag{16}$$

The equations relate the stress $\mathbf{T}$, body force $\mathbf{f}$, and particle displacement $\mathbf{u}$ in the elastic material. We note in passing the occasional use of the *momentum density* ($[\text{M}][\text{L}]^{-2}[\text{T}]^{-1}$) in the literature, defined as $\mathbf{p} = \rho \mathbf{v}$ where $\mathbf{v} = \frac{\partial}{\partial t} \mathbf{u}$, so that

$$\nabla \cdot \mathbf{T} + \mathbf{f} = \frac{\partial \mathbf{p}}{\partial t}. \tag{17}$$

38

From the strain (**S**)-displacement (**u**) relationship, noting $\nabla_s = \left(\nabla + \nabla^T \right)$ is the symmetric gradient operator and $(\cdot)^T$ is the transpose operator,

$$\nabla_s \mathbf{u} = \mathbf{S} \Rightarrow \nabla_s \mathbf{v} = \frac{\partial \mathbf{S}}{\partial t} \tag{18}$$

using a time derivative on both sides.

For a standard elastic solid, the strain is the stress multiplied by the compliance or $\mathbf{S} = \mathbf{s} : \mathbf{T}$, with : as the double-dot product, and so

$$\frac{\partial \mathbf{S}}{\partial t} = \mathbf{S} : \frac{\partial \mathbf{T}}{\partial t} \Rightarrow \nabla_s \mathbf{v} = \mathbf{S} : \frac{\partial \mathbf{T}}{\partial t}, \tag{19}$$

where $\mathbf{v} = d/dt(\mathbf{u})$ is the particle velocity, producing

$$\mathbf{c} : \nabla_s \mathbf{v} = \frac{\partial \mathbf{T}}{\partial t}. \tag{20}$$

Here we also use the definition of the stiffness **c** such that $\mathbf{c} : \mathbf{s} = \boldsymbol{\delta}$, with $\boldsymbol{\delta}$ as the identity tensor. If we take $\nabla \cdot \mathbf{T} + \mathbf{f} = \rho \frac{\partial}{\partial t} \mathbf{v}$ and take its derivative with respect to time, t,

$$\nabla \cdot \frac{\partial \mathbf{T}}{\partial t} + \frac{\partial \mathbf{f}}{\partial t} = \rho \frac{\partial^2}{\partial t^2} \mathbf{v} \Rightarrow$$

$$\nabla \cdot (\mathbf{c} : \nabla_s \mathbf{v}) + \frac{\partial \mathbf{f}}{\partial t} = \rho \frac{\partial^2}{\partial t^2} \mathbf{v} \Rightarrow$$

$$\nabla_{i\alpha} c_{\alpha\beta} \nabla_{\beta j} v_j + \frac{\partial}{\partial t} f_i = \rho \frac{\partial^2}{\partial t^2} v_i, \tag{21}$$

the equation of motion in component form, written in terms of the particle velocity v_i, stiffness $c_{\alpha\beta}$, and the body force f_i. In this form, we have chosen to abbreviate the component notation

39

625 by taking advantage of the inherent symmetry present in even a very anisotropic material, such

626 that the full fourth-order stiffness tensor c_{ijkl} may be written as $c_{\alpha\beta}$ where $\alpha, \beta \in \{1, 2, \ldots, 6\}$.

c. *Assuming a harmonic propagating wave*

628   Suppose we have a harmonic wave, an acoustic wave propagating along $\mathbf{e}_\eta = a_1\mathbf{e}_1 + a_2\mathbf{e}_2 +$

629 $a_3\mathbf{e}_3$, and assume the unit vectors $\mathbf{e}_i$ form a right-handed orthogonal coordinate system. Then

630 the terms in eqn. (21) will be proportional to $e^{\iota(\omega t - k(\mathbf{e}_\eta \cdot \mathbf{r}))}$.

631   This lets us greatly simplify the operators $\nabla_{i\alpha}$ and $\nabla_{\beta j}$, replacing them, respectively, with

632 matrices

$$\iota k \begin{bmatrix} a_1 & 0 & 0 & 0 & a_3 & a_2 \\ 0 & a_2 & 0 & a_3 & 0 & a_1 \\ 0 & 0 & a_3 & a_2 & a_1 & 0 \end{bmatrix} \equiv \iota \mathfrak{k}_{i\alpha} k \equiv \iota k_{i\alpha} \tag{22}$$

633 and

$$\iota k \begin{bmatrix} a_1 & 0 & 0 \\ 0 & a_2 & 0 \\ 0 & 0 & a_3 \\ 0 & a_3 & a_2 \\ a_3 & 0 & a_1 \\ a_2 & a_1 & 0 \end{bmatrix} \equiv \iota \mathfrak{k}_{\beta j} k \equiv \iota k_{\beta j}. \tag{23}$$

40

634 If we set the applied forces, $f_i = 0 \forall i \in \{1, 2, 3\}$, then $\nabla_{i\alpha} c_{\alpha\beta} \nabla_{\beta j} v_j + \frac{\partial}{\partial t} f_i = \rho \frac{\partial}{\partial t} v_i$ becomes

$$-k^2 \mathfrak{k}_{i\alpha} c_{\alpha\beta} \mathfrak{k}_{\beta j} v_j = -\rho \omega^2 v_i. \tag{24}$$

635 By defining the *Christoffel matrix* $\Gamma_{ij} \equiv \mathfrak{k}_{i\alpha} c_{\alpha\beta} \mathfrak{k}_{\beta j}$,

$$k^2 \Gamma_{ij} v_j = \rho \omega^2 v_i. \tag{25}$$

636 From the *Christoffel equation* (25) we may obtain $(k^2 \Gamma_{ij} - \delta_{ij} \rho \omega^2) v_j = 0$, the *slowness equation*.

637 Little more can be done to solve this equation without knowing the details of the material's

638 anisotropy, but let us consider the simplest case here.

639 ***d. In an isotropic medium produces the expected relationship between the particle velocity and***

640 ***the strain***

641 Let us presume the wave is in an isotropic medium, noting that $c_{12} = \frac{1}{2}(c_{11} - c_{44})$ and the

642 substantial symmetry present in the media otherwise, leaving only two independent constants

643 to define it.

644 The Christoffel matrix becomes

$$[\Gamma_{ij}] = [\mathfrak{k}_{i\alpha}][c_{\alpha\beta}][\mathfrak{k}_{\beta j}] = \begin{bmatrix} c_{11} a_1^2 + c_{44}(1 - a_1^2) & (c_{12} + c_{44}) a_1 a_2 & (c_{12} + c_{44}) a_1 a_3 \\ (c_{12} + c_{44}) a_2 a_1 & c_{11} a_1^2 + c_{44}(1 - a_2^2) & (c_{12} + c_{44}) a_2 a_3 \\ (c_{12} + c_{44}) a_3 a_1 & (c_{12} + c_{44}) a_3 a_2 & c_{11} a_3^2 + c_{44}(1 - a_3^2) \end{bmatrix} \tag{26}$$

41

645 Suppose we assume that the wave is propagating along $\mathbf{e}_3$. Since the material is isotropic,

646 it does not matter which direction we choose. Then $\mathbf{e}_\eta = 0\mathbf{e}_1 + 0\mathbf{e}_2 + 1\mathbf{e}_3$ and $\mathbf{k} = k\mathbf{e}_\eta = k\mathbf{e}_3$:

647 $k^2 \Gamma_{ij} v_j = \rho\omega^2 v_i$ becomes

$$k^2 \begin{bmatrix} c_{44} & 0 & 0 \\ 0 & c_{44} & 0 \\ 0 & 0 & c_{11} \end{bmatrix} \begin{bmatrix} v_1 \\ v_2 \\ v_3 \end{bmatrix} = \rho\omega^2 \begin{bmatrix} v_1 \\ v_2 \\ v_3 \end{bmatrix} \tag{27}$$

648 and so $k^2 c_{44} v_1 = \rho\omega^2 v_1$, $k^2 c_{44} v_2 = \rho\omega^2 v_2$, and $k^2 c_{11} v_3 = \rho\omega^2 v_3$.

649 A shear wave is propagating along $\mathbf{e}_3$ with $\mathbf{v} = \mathbf{e}_1 v_1 e^{\iota(\omega t - k x_3)}$ where x_i is a coordinate along

650 $\mathbf{e}_i$ that must have $k^2 c_{44} = \rho\omega^2$. Likewise, another shear wave exists such that $\mathbf{v}' = \mathbf{e}_2 v_2 e^{\iota(\omega t - k x_3)}$

651 with $k^2 c_{44} = \rho\omega^2$. Finally, $\mathbf{v}'' = \mathbf{e}_3 v_3 e^{\iota(\omega t - k \chi_3)}$ with $k^2 c_{11} = \rho\omega^2$ as the longitudinal wave. These

652 bulk waves have different speeds depending on c_{44} and c_{11}.

653 Now it is useful to note the particle displacement $\mathbf{u}$ can be found through integration of the

654 particle velocity $\mathbf{v}$,

$$\mathbf{u} = \int \mathbf{v}\, dt = \frac{v}{\iota\omega} e^{\iota(\omega t - k x_3)} \mathbf{e}_3, \tag{28}$$

655 and so the resulting strain along the $\mathbf{e}_3$ direction is

$$S_{33}\mathbf{e}_3 = \frac{\partial \mathbf{u}}{\partial z}\mathbf{e}_3 = -\frac{vk}{\omega} e^{\iota(\omega t - k x_3)} \mathbf{e}_3. \tag{29}$$

656 Since

$$\frac{vk}{\omega} = \frac{2\pi v}{2\pi f \lambda} = \frac{v}{f\lambda} = \frac{v}{c_0} \tag{30}$$

42

657 where c_0 is the speed of sound, we find that the magnitude of the longitudinal strain is a ratio

658 of the particle velocity to the speed of sound in the media for the longitudinal wave described

659 by $\mathbf{v}''$,

$$|S_{33}| = \frac{vk}{\omega} = \frac{v}{c_0}. \tag{31}$$

660 The shear wave solutions will produce similar results.

661 **3. Schematic of Experimental Setup for Surface Acoustic Wave Particle Velocity Measurement**